Astron. Astrophys. 333, 264–268 (1998)

ASTRONOMY
AND
ASTROPHYSICS

Extended red emission (ERE) detected in the 30 Doradus nebula⋆

S. Darbon, J.-M. Perrin, and J.-P. Sivan

Observatoire de Haute Provence du CNRS, F-04870 Saint Michel l'Observatoire, France

Received 21 August 1997 / Accepted 17 December 1997

Abstract. We present low-dispersion visible spectra of two regions of the 30 Doradus nebula. When corrected for atomic continuum emission and divided by the spectrum of the exciting and illuminating stars, one of the two spectra clearly shows Extended Red Emission (ERE) superimposed on the scattering component. This ERE band peaks around 7270 Å and is 1140 Å width. HAC grains are found to explain the observed spectra in terms of scattering and luminescence.

Key words: ISM: individual objects: 30 Dor (LMC) – galaxies: Magellanic Clouds – galaxies: ISM – ISM: dust, extinction – ISM: lines and bands

1. Introduction

Spectrophotometric studies have revealed the presence of a wide emission band in the red part of the continuous spectrum of several types of galactic objects: reflection nebulae (Witt & Boroson 1990), planetary nebulae (Furton & Witt 1992), HII regions (Sivan & Perrin 1993) and high latitude cirrus (Guhathakurta & Tyson 1989); this band, called Extended Red Emission (ERE), consists of a broad emission bump about 1000 Å wide (FWHM), centered between 6000 and 8000 Å. In order to explain this emission, two hypotheses are generally invoked: Poincaré fluorescence of isolated Polycyclic Aromatic Hydrocarbons (PAH) molecules (d'Hendecourt et al. 1986, Léger et al. 1988) or fluorescence from solid state materials such as filmy Quenched Carbonaceous Composite (f-QCC) (see e.g. Sakata et al. 1992) or Hydrogenated Amorphous Carbon (HAC) (see e.g. Watanabe et al. 1982, Furton & Witt 1993).

In order to better characterize the mechanisms responsible for ERE, we have thought it useful to observe objects in which the physical and chemical conditions are distinct from those encountered in galatic nebulae. This has led us to observe the dusty halo of the galaxy M82 in the spectrum of which we have detected an ERE band (Perrin et al. 1995). Also, we have observed HII regions in the Magellanic Clouds because the interstellar medium of these galaxies shows a lower metallicity than the interstellar medium of our Galaxy (Russell & Dopita 1990). Moreover, their proximity make them well suited for detailed studies. In this paper, we present the results obtained on the well-studied starburst nebula 30 Doradus in the Large Magellanic Cloud (LMC). This supergiant HII region has a bright core of 200 pc in diameter with filaments outlying over 2 kpc. Its morphology and dynamics are very peculiar (Elliott et al. 1977, Cox & Deharveng 1983). Its stellar content is uncommon; in particular, the R136 cluster is rich in WR and early type O stars and releases almost 50% of the ionizing flux in the nebula (Walborn 1984, Melnick 1985).

The observations and data reductions are described in the next section. Sect. 3 presents the main spectrophotometric results we have interpreted in terms of dust scattering and fluorescence.

2. Observations and data reduction

Spectra of the 30 Doradus nebula in the LMC were obtained in November 1994 using the Boller & Chivens long slit spectrograph equiped with a Fairchild CCD (FA 2048L) and mounted at the Cassegrain focus of the European Southern Observatory 1.52 m telescope in La Silla. The spectral domain of interest [3800 Å,9300 Å] was covered with a mean dispersion of 250 Å mm^{-1}. The usable slit length on the sky was 226" (276 pixels on the detector), the slit width was set to 3", which corresponds to a spectral resolution of 13.7 Å. A single slit position (position angle of 77°) was observed on the nebula. It was centered 57" north of R136 (Fig. 1). We made a number of short exposures, alternatively on the nebula and on the surrounding sky background located 93' north-east from the position on the nebula. As discussed previously (Perrin & Sivan 1992), this procedure avoids the saturation of the CCD with bright nebular emission lines and allows a fine monitoring of the continuous spectrum of the night-sky background. The following sequence was taken up: 1 exposure of 120 s on the sky background + 1 exposure of 240 s on the nebula + another exposure of 120 s on the sky background. A total exposure time of 960 s was obtained on the nebula. The exciting and illuminating cluster R136 and the surrounding brightest stars D, C, W, F, A and E (which are thought to contribute to the illumination of the nebula), as quoted in Fig. 1, were observed near the meridian in

Send offprint requests to: J.-P. Sivan

⋆ Based on observations made at the European Southern Observatory (ESO), La Silla (Chile)

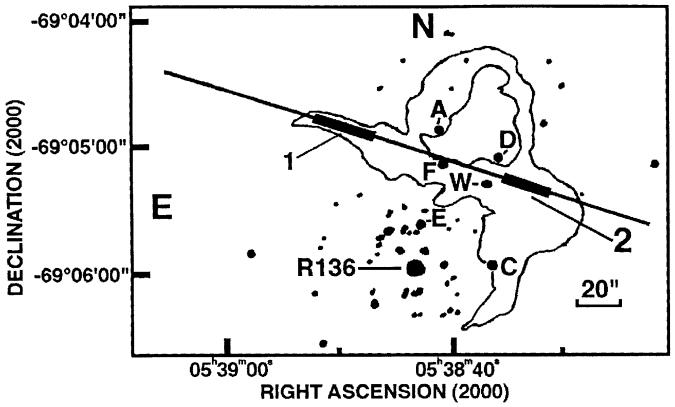

Fig. 1. Spectrophotometric observations of the 30 Doradus HII region: schematic representation of the position of the spectrograph slit. Regions 1 and 2 for which one-dimensionnal spectra were extracted are shown. The ionizing and illuminating sources are indicated: R136, D, C, W, F, A and E, as labelled by Melnick (1983)

order to compare their spectral energy distribution with that of the nebula. The standard star LTT377 (Hamuy et al. 1992) was observed for flux calibration.

Data reduction was conducted at Observatoire de Haute Provence using MIDAS software on a DEC-ALPHA computer. After co-adding the short exposure frames, offset subtracting and flat-fielding, the spectrum was spatially divided into two bins which correspond to two different parts of the nebula (free of contamination by stellar spectra) and one-dimensionnal spectra were extracted for these two regions. Region 1 is located 33" east and 67" north from R136 and its dimensions are 28"×3"; region 2 is located 52" west and 38" north from R136 and its dimensions are 22"×3" (Fig. 1). Then, each one-dimensionnal spectrum was wavelength- and flux-calibrated. Atmospheric extinction correction was applied using the standard extinction curve of La Silla. Sky subtraction was done by removing from a nebular spectrum the corresponding sky background spectrum extracted by binning the same pixels along the spectrograph slit (in order to avoid any instrumental function effect). The spectrum of each exciting star was reduced as above except for the sky subtraction: we subtracted a mean sky background taken on each side of the star spectrum on the same frame.

In the visible range, the LMC interstellar reddening curve (Nandy et al. 1981, Morgan & Nandy 1982) does not differ from the standard curve (Prévot et al. 1984, Howarth 1983, Pei 1992). So, the spectra were dereddened using the LMC curve and values of the interstellar extinction were measured globally to take account of the galactic and LMC interstellar extinction. We applied the classical formula that gives the nebular intensity $I_o(\lambda)$ relative to Hβ corrected for interstellar extinction as a function of the observed intensity I(λ) and the observed Hβ intensity I(Hβ):

$$I_o(\lambda)/I_o(H\beta) = [I(\lambda)/I(H\beta)]10^{C(H\beta)f(\lambda)} \quad (1)$$

C(Hβ) and f(λ) are respectively the reddening correction at Hβ and the reddening function. For the two regions on the nebula, C(Hβ) was derived from the comparison of the observed Hδ/Hβ, P9/Hβ and P11/Hβ ratios with the theoretical ratios computed by Brocklehurst (1971) under case B conditions. We obtained C(Hβ)=0.58 for region 1 and C(Hβ)=0.35 for region 2. We note that these values compare well with those found by Mathis et al. (1985). For R136, we used the value C(Hβ)=0.49 from Fitzpatrick & Savage (1984).

For each region, we have calculated the atomic continuum emission, normalized to Hβ, supposing a pure hydrogen nebula; since $N(He^+)/N(H^+) \approx 0.082$ (Rosa & Mathis 1987), the He contribution can be neglected. The continuous atomic spectrum is the sum of the two-photon decay emission and of the free-bound continuum radiation and it is a function of the electron temperature and of the electron density. We measured the electron temperature and the electron density in a classical way, using respectively the [NII] and [SII] lines intensity ratios. We found T_e=10250 K and n_e=800 cm^{-3} for region 1 and T_e=11600 K and n_e=200 cm^{-3} for region 2. The HI recombination continuous emission and the HI two-photon continuum were calculated using the formulae given by Brown & Mathews (1970). To calculate the first component we used the HI continuous emission coefficient obtained using a spline interpolation from the data of Brown & Mathews (1970). For the calculation of the second component we used the effective recombination coefficient for populating the 2^2S level of HI and the collisional transition rate for HI 2^2S, 2^2P, both interpolated for the same temperature from the same data. The total continuum spectrum was normalized to the intensity of the Hβ line. Also, to avoid artifact in the subtraction of the atomic continuum, we convolved the theoretical spectrum with the instrumental function (i.e., a 13.7 Å window) from 8199 to 8447 Å, thus taking into account the instrumental blend of the Paschen lines down to Pa18. The intensity of the Paschen lines was calculated relative to the intensity of the Hβ line, using the formula given by Goldwire (1968). Figs. 2a and 2b show the dereddened spectra for respectively regions 1 and 2. The calculated atomic continuous spectra are superimposed in dotted line.

To characterize the scattering and, eventually, the luminescence phenomena, we have compared the color of the nebula spectra to that of the illuminating source spectrum. For this purpose, we have divided the dereddened spectra of regions 1 and 2, corrected for atomic continuum emission, by the sum of the dereddened spectra of R136 and of the surrounding brightest stars D, C, W, F and A. The resulting spectra are displayed in Figs. 2c and 2d. In what follows, we shall refer to them as *reduced spectra*. As shown by Hill et al. (1993), stars in the close vicinity of R136 have very low nebular extinction ($E(B-V) < 0.03$). As a result, the reddening between the illuminating sources and regions 1 and 2 is negligeable and the reduced spectra in Figs. 2c and 2d do reveal the scattering and luminescence properties of the nebular dust.

3. Results and discussion

These spectra appear to be basically red over the entire 4000-9000Å wavelength range. This can be simply explained by a

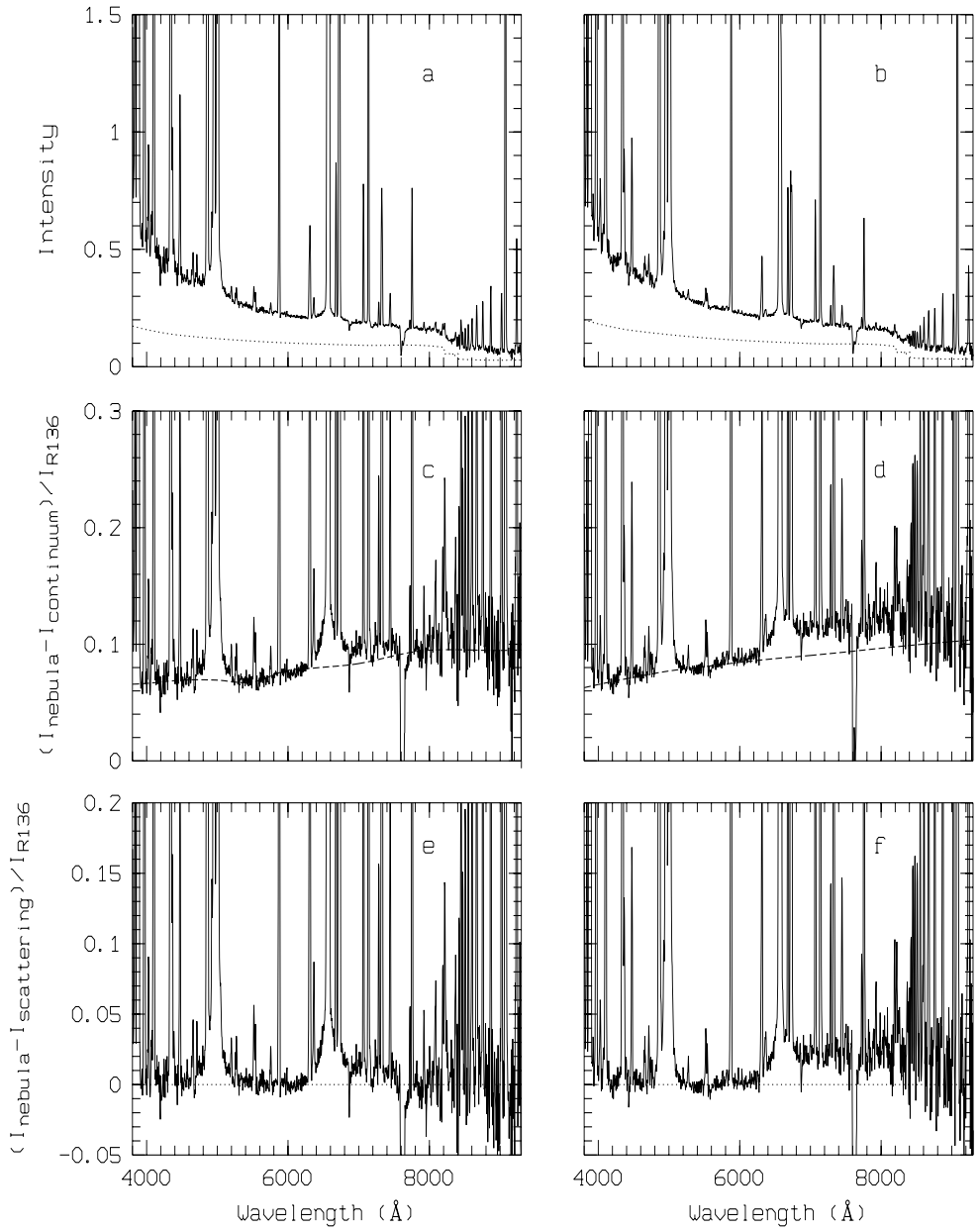

Fig. 2. a and **b** Spectra of, respectively, region 1 and region 2 of 30 Doradus; the theoretical atomic spectrum is superimposed in dotted line (Intensity unit: **a** 10^{-13}erg cm^{-2} Å^{-1} s^{-1} arsec^{-2}, **b** 10^{-12}erg cm^{-2} Å^{-1} s^{-1} arsec^{-2}). **c** and **d** Division of the nebula spectrum corrected for the atomic continuous emission by the spectrum of the exciting stars; theoretical scattering spectra are superimposed in dashed line. **e** and **f** Subtraction from the observed scattering spectra of theoretical scattering spectrum. The strong absorption A band of O_2 is apparent in all spectra around 7620Å.

significant contribution to scattering from dust particles whose size parameter is greater than 1. According to Lamy & Perrin (1997), radiation pressure acts more efficiently on submicronic grains than gravitational attraction does. But this is not the case for micron-sized grains. So, in the neighbourhood of early-type stars, in particular in the region surrounding R136, submicronic grains are expelled, leading to a decrease of the grain density and to an increase of the relative abundance of large grains. This is in good agreement with the weak internal extinction observed by Hill et al. (1993).

We have tried to model the scattering component in each reduced spectrum. For this purpose, we have studied scattering of light by grains for a large number of materials which are real materials of astrophysical interest: silicates (olivine, andesite, augite,...), metals (iron, nickel), iron sulphides (pyrrhotite, troilite), organic materials (tholins, icetholin, kerogen, poly-HCN), glassy carbon, amorphous carbons, graphite, a lot of HACs (whose properties depend on the conditions of synthesis), silicon carbides and meteoritic materials. Calculations were conducted in the framework of single scattering (justified by small values of optical depth in the observed regions) for several grain size distributions and several scattering angle intervals. We retained only spectra that (i) fit the observed ones at least in their bluest ($\lambda \,.\, 5500$Å) and reddest ($\lambda \,\&\, 8500$Å) parts, and (ii) change only smoothly when scattering parameters are slightly modified (i.e. stationnary solutions). Among all the calculated spectra, only those obtained with HAC grains proved to fit satisfactorily the observed scattering components.

For region 1, the best fit (Fig. 2c) was obtained for HAC grains (i) which have undergone a very low bombardment by ions and electrons during their formation, (ii) which have never been submitted to high temperature and (iii) for which minimal adsorption of hydrogen atoms has occured. Fig. 2e shows the observed reduced spectrum after subtraction of the theoretical component. The ERE band does not appear very clearly: if it exists, it should be extremely faint. The fit is obtained using the complex indexes of refraction given by McKenzie et al. (1983), a maximum particle radius of 0.5 μm, a value of 2.9 for the exponent p of the size distribution ($\propto a^{-p}$ where a is the radius of the particle) and a wide interval of scattering angle ($\simeq$ [10°,170°]). This value of p, which is lower than those found in the diffuse interstellar medium ($p \simeq 3.5$), is in agreement with the relative abundance of micron-sized grains.

For region 2, we have found that the best fit to the scattering component was given (Fig. 2d) by a model using HAC grains submitted to high ionic bombardment and high hydrogen excess during their formation. The fit is obtained using the complex indexes of refraction given by Khare et al. (1987), a p value of 1.5, a maximum particle radius of 1.5 μm and a small scattering angle range ($\simeq$ [75°,105°]). In this case, an ERE band is unambiguously detected (Fig. 2f). It looks similar to those found in galactic HII regions (Perrin & Sivan 1992, Sivan & Perrin 1993), with a peak wavelength of 7270 Å and a width of 1140 Å (FWHM). The ratio of integrated ERE intensity in the 6000-9000 Å range to the scattered light intensity is 0.20 ± 0.05. This value is in the average of those found in reflection nebulae (Witt & Boroson 1990).

The location of region 1 relative to R136 and the other luminous stars (Fig. 1) is fundamentally unknown but is not incompatible with the wide range of scattering angle needed to fit the observed scattering component: we can suppose that most of the stars contribute to the illumination of this region. On the contrary, the narrow angular range used for region 2 suggests a contribution from a smaller number of illuminating stars. This range being centered at 90°, the observed color of the scattered light appears redder than it would be if the scattering angular range was wider (Witt 1985, Perrin & Lamy 1989). Consequently, the intrinsic values of p and of the maximum particle radius should be respectively greater and lower than those of our fit. It should be noted that color effects can also be induced by surface roughness of grains (Perrin & Lamy 1989).

The properties of HACs, in particular their optical properties, depend on the conditions of preparation (see e.g. Watanabe et al. 1982, McKenzie et al. 1983, Khare et al. 1987) and on the radiative, ionic, atomic and/or molecular processings that follow their formation (see e.g. Furton & Witt 1993). When submitted to UV radiations, these materials exhibit luminescence phenomena, whose intensity is releated to the UV illumination conditions and to the efficiency of rehydrogenation of the grains (Duley et al. 1997).

Accounting for ERE by luminescence from HAC grains, our results appear to be self-consistent on the basis of laboratory results, in the sense that ERE is found to be relatively bright in a region where the scattering is explained by highly hydrogenated HAC grains, and, on the contrary, ERE is absent (or barely detected) in a region where the scattering is accounted for by poorly hydrogenated HAC grains.

Also, our results suggest that astrophysical conditions should significantly differ from one region to the other. This is probably the case, since hydrogen molecules are present in region 1 and absent in region 2, according to the H_2 emission map of Poglitsch et al. (1995). ERE is found in a region where H_2 is absent and inversely. This result agrees well with the finding of Field et al. (1994) and Lemaire et al. (1996) who did not observe any clear correlation between ERE intensity and H_2 emission in NGC 2023 and NGC 7023.

For the two observed regions, HAC grains are invoked to explain the scattering and luminescence components. We think that the presence of such carbonaceous grains in the LMC interstellar medium is supported by the two following facts:
(i) In the LMC, the stellar carbon abundance and, in particular, the stellar C/O abundance ratio are entirely normal but the HII regions appear to be overdeficient in carbon and have a C/O ratio lower than that observed in the Galaxy (Russel & Dopita 1992). This suggests that a substantial fraction of the interstellar carbon might be in the grains, in agreement with the good spatial correlation observed between the emission of CO, C^+ and the dust thermal emission in the far infrared (Poglitsch et al. 1995).
(ii) A very weak ultraviolet extinction bump is observed in the 30 Doradus region (Fitzpatrick 1988). As shown by Colangeli et al. (1993), HAC grains do not exhibit an extinction feature at 2175 Å.

4. Conclusion

We have observed the continuous spectrum of two regions in the core of the 30 Doradus nebula. ERE is unambiguously revealed for one of the two regions and is at the limit of detection for the other region. This is the first detection of ERE in an extragalactic HII region.

The differences in the observed spectra cannot be accounted for by variation in the internal extinction across the nebula: it has been shown by Hill et al. (1993) that extinction is almost negligeable in the central part of the 30 Doradus nebula, a finding which is in good agreement with the morphology and the dynamics of the nebula.

HAC grains can explain the observed spectra in terms of scattering and luminescence: highly hydrogenated HAC grains and poorly hydrogenated HAC grains are invoked respectively for the region where ERE is clearly visible and the region where ERE is not obviously seen. This difference in grains properties is in good agreement with the difference in the astrophysical conditions prevailing in the two regions.

Acknowledgements. We wish to thank the referee, Pr. A. Witt, for helpful comments.

References

Brocklehurst, M., 1971, MNRAS 153, 471
Brown, R.L., Mathews, W.G., 1970, ApJ 160, 939
Colangeli, L., Mennella, V., Blanco, A., Fonti, S., Bussoletti, E., Gumlich, H.C., Jung, CH., 1993, ApJ 418, 435
Cox, P., Deharveng, L., 1983, A&A 117, 265
d'Hendecourt, L.B., Léger, A., Olofsson, G., Schmidt, W., 1986, A&A 170, 91
Duley, W.W., Seahra, S., Williams, D.A., 1997, ApJ 482, 866
Elliott, K.H., Goudis, C., Meaburn, J., Tebbutt, N.J., 1977, A&A 55, 187
Field, D., Gerin, M., Leach, S., Lemaire, J.L., Pineau des Forêts, G., Rostas, F., Rouan, D., Simons, D., 1994, A&A 286, 909
Fitzpatrick, E.L., Savage, B.D., 1984, ApJ 279, 578
Fitzpatrick, E.L., 1988, in I.A.U. Symp. 135, Interstellar Dust, eds L.J. Allamandola and A.G.G.M. Tielens, p. 37
Furton, D.G., Witt, A.N., 1992, ApJ 386, 587
Furton, D.G., Witt, A.N., 1993, ApJ 415, L51
Goldwire, H.C., 1968, ApJS 17, 445
Guhathakurta, P., Tyson, J.A., 1989, ApJ 346, 773
Hamuy, M., Walker, A.R., Suntzeff, N.B., Gigoux, P., Heathcote, S.R., Phillips, M.M., 1992, PASP 104, 533
Hill, J.K., Bohlin, R.C., Cheng, K.-P., Fanelli, M.N., Hintzen P., O'Connell, R.W., Roberts, M.S., Smith, A.M., Smith, E.P., Stecher, T.P., 1993, ApJ 413, 604
Howarth, I.D., 1983, MNRAS 203, 301
Khare, B.N., Sagan, C., Thompson, W.R., Arakawa, E.T., Votaw, P., 1987, J. Geophys. Res. 92, 15067
Lamy, P.L., Perrin, J.-M., 1997, A&A 327, 1147
Léger, A., Boissel, P., d'Hendecourt, L., L.1988, Phys. Rev. Lett. 60, 921
Lemaire, J.L., Field, D., Gerin, M., Leach, S., Pineau des Forêts, G., Rostas, F., Rouan, D., 1996, A&A 308, 895
McKenzie, D.R., McPhedran, R.C., Savvides, N., Botten, L.C., 1983, Philosophical Magazine B48, 341
Mathis, J.S., Chu, Y.-C., Peterson, D.E., 1985, ApJ 292, 155
Melnick, J., 1983, The Messenger No. 32, 11
Melnick, J., 1985, A&A 153, 235
Morgan, D.H., Nandy, K., 1982, MNRAS 199, 979
Nandy, K., Morgan, D.H., Willis, A.J., Wilson, R., Gondhalekar, P.M., 1981, MNRAS 196, 955
Pei, Y.C., 1992, ApJ 395, 130
Perrin, J.-M., Lamy, P.L., 1989, A&A 226, 288
Perrin, J.-M., Sivan, J.-P., 1992, A&A 255, 271
Perrin, J.-M., Darbon, S., Sivan, J.-P., 1995, A&A 304, L21
Poglitsch, A., Krabbe, A., Madden, S.C., Nikola, T., 1995, ApJ 454, 293
Prévot, M.L., Lequeux, J., Maurice, E., Prévot, L., Rocca-Volmerange, B., 1984, A&A 132, 389
Rosa, M., Mathis, J.S., 1987, ApJ 317, 163
Russell, S.C., Dopita, M.A., 1990, ApJS 74, 93
Russel, M., Dopita, M.A., 1992, ApJ 384, 508
Sakata, A., Wada, S., Narsawa, T., Asano, Y., Iijima, Y., Onaka, T., Tokunaga, A.T., 1992, ApJ 393, L83
Sivan, J.-P., Perrin, J.-M., 1993, ApJ 404, 258
Walborn, N.R., 1984, in I.A.U. Symp. 108, Structure and Evolution of the Magellanic Clouds, eds S. Bergh and K. Boer, p. 243
Watanabe, J., Hasegawa, S., Kurata, Y., 1982, Japanese Journal of Applied Physics 21, 856
Witt, A.N., 1985, ApJ 294, 216
Witt, A.N., Boroson, T.A., 1990, ApJ 355, 182